Single-walled carbon nanotube structure and radiation defects under the high energy electron beam

M.Yu. Tashmetov, I.I. Yuldashova*

Institute of Nuclear Physics, Academy of Sciences of Uzbekistan, Mirzo Ulugbek district, Ulugbek township, Khorasan 1, 100214, Tashkent, Uzbekistan

Received 29.08.2021

* Corresponding author: e-mail iroda@inp.uz, Phone: +998909972114

Исследовано влияние электронного облучения до флюенса 1.54×10^{17} электрон/см^2 на структурные параметры, размеры нанокристаллитов, микронапряжения и спектры комбинационного рассеяния однослойной углеродной нанотрубки (ОСУНТ). Облучение электронами приводит к увеличению параметров решетки в направлениях a и b от 4.7623 до 4.9378 Å и уменьшению по оси c от 3.9491 до 3.9469 Å. Электронное облучение стимулирует рост размера нанокристаллитов от 4.06 нм до 5.03 нм, приводит к сдвигу спектров комбинационного рассеяния в сторону более высоких частот и указывает на появление спектра 805 см$^{-1}$, вызванного образованием дефектов в ОСУНТ.

Ключевые слова: однослойные углеродные нанотрубки, электронный пучок, Раманская спектроскопия, рентгеноструктурный анализ, параметры ячейки.

The effect of electron irradiation up to fluence of 1.54×10^{17} electron/cm^2 on the structural parameters, sizes of nanocrystallites, microstrains, and Raman spectra of a single-walled carbon nanotube (SWCNT) was studied. Electron irradiation leads to an increase in the lattice parameters in the *a* and *b* directions from 4.7623 Å to 4.9378 Å and a decrease along the *c* axis from 3.9491 Å to 3.9469 Å. Electron irradiation stimulates the growth of the nanocrystallite size from 4.06 nm to 5.03 nm, leads to a shift of the Raman spectra towards higher frequencies, and indicates the appearance of a spectrum at 805 cm^{-1}, which is caused by the formation of defects in a SWCNT.

Keywords: Single-walled carbon nanotubes, e-beam, Raman spectroscopy, XRD – analysis, cell parameters.)

https//doi.org/10.52304/.v23i2.237

I. Introduction

A carbon nanotube is a convenient model object with a simple structure, known locations and bonds of carbon atoms, metallic and (or) semiconducting conductivity. The results of a detailed study of a single-walled carbon nanotube make it possible to use them in the study of more complex multicomponent nanocompounds, in which nitrogen, oxygen, hydrogen atoms, and sometimes heavier atoms are "incorporated-present" as impurities. Distortions introduced by impurity atoms lead to a change in the binding energy, displacement of carbon atoms from the ideal position, and can also initiate a change in symmetry.

Based on the relationship between the structure and properties of materials [1], it can be assumed that the introduction of defects (distortion, substitution) into a single-walled carbon nanotube (SWCNT) will lead to a change in its properties. It should be noted that the same changes can be made to the structure of a SWCNT under external influence (temperature,

pressure and irradiation). In some cases, exposure to radiation is the optimal and controllable way to study the formation of defects and their effect on symmetry, on the radial and tangential vibrations of carbon atoms, on the structure and properties of a carbon nanotube (CNT).

The structure of a SWCNT was investigated from the very beginning of its preparation [2], in which the existence of a unit cell with a hexagonal structure was revealed. In many samples, along with a SWCNT, graphite and impurities of metal catalysts are present.

The physical and chemical properties diversity of carbon nanomaterials are determined by the possibility of influencing their structure, as well as the generation of different defects [3, 4]. At [4] details the radiation defects that result from neutron flux and gamma irradiation exposure in the SWCNT. In it, the samples were irradiated with neutrons to 1.28×10^{17} n/cm^{2}fluence and with gamma rays to 1.54×10^{17} ph/cm^2 fluence.

One of the methods to change properties of SWCNT is to generate radiation defects as a result of electron beam exposure. Electron bombardment is capable of creating radiation point defects, in contrast to the irradiation by low-energy photons, which are mainly used to excite π-electron systems, and can lead to the polarization of the molecules of the nanostructures. The electron irradiation of SWCNT is not only caused radiation defects, which will contribute to the degradation of nanotubes, herewith the crosslinking appears due to the ruptured bonds and generation of vacancies.

The structure, topology, and size of CNTs are a source of their outstanding mechanical and optical properties and their electronic behavior. Raman spectroscopy is a valuable technique for determining the diameter distribution, chirality, purity, and architecture of CNTs [3-19]. Vibrational properties, electronic structures, quality of the samples and diameter characterization of the various carbon materials can be analyzed by the Raman spectroscopy including SWCNT, double-walled (DWCNT) [9] and multi-walled (MWCNT) carbon nanotubes [3, 4, 17]. Changes in SWCNTs properties under irradiation with protons of various energies (1~18 MeV) and doses (3.0×10^{-7} ~ 2.2×10^{-2} nC/μm^2) were studied in [18] by using Raman spectroscopy. After the high-energy proton irradiation (~18 MeV) no significant change in Raman spectra was observed, however, after low-energy proton irradiations (1~6 MeV) some of the semiconducting SWCNTs exhibited irradiation induced damage.

The most prominent Raman features in SWCNTs are the radial breathing modes (RBMs), the higher frequency D (disordered), G (graphite) and G′ (second-order Raman scattering from D-band variation) modes [3]. Although the D, G, and G′ modes are found in graphite, the RBM is specific to SWCNT and is representative of the isotropic radial expansion of the tube.

Authors of [5] reported about the influence of low energy e-beam (at 1 kV for 1 min, dosage 2.3×10^{21} to 3.1×10^{21} electron/cm^{-2}) focused on the single-walled carbon nanotube. After studying the effect of low-energy (100 keV) electron beam on the deposited hydrocarbon EBID and amorphous carbon during the synthesis of SWNTs, they concluded that the increase in D-mode electron beam in Raman spectra is mainly due to amorphous rather than structural damage of SWNTs. Authors of [20] found that SWCNTs exposed to focused electron beam were severely deformed locally and neck-like features were developed along the tube due to the removal of carbon atoms by knock-on displacements.

There are very few X-ray diffractometry (XRD) studies of carbon nanotubes so far, especially, SWCNTs and XRD analysis after the electron irradiation effects.

It follows from the above literature data that although the effect of gamma rays, protons, electrons, and ions on a SWCNT has been studied [10, 21, 22], a comprehensive study of the structure, microstress, atomic vibrations, nanotube diameter, and nanocrystallite size under electron irradiation of various fluencies has not been practically investigated. The purpose of the work is to determine the structure of SWCNT and to study radiation defects under exposure to high fluency of 2 MeV electron beam.

II. Experimental methods

We have used SWCNT nanopowder samples ($D\times L$ – 1.2–1.5 nm×2–5 μm) produced by Electric Arc Discharge method at Sigma-Aldrich.

The samples were irradiated at the liner electron accelerator Electronics-U003 at the Institute of Nuclear Physics, Uzbekistan at the following e-beam parameters: electron energy 2 MeV, current density 0.17 μA/cm^2. The choice of such a value for the energy and current density of the electron beam is as-

© Academy of Sciences of Republic of Uzbekistan, 2021

sociated with the aim of avoiding heating of the sample, which leads to the appearance of an air impurity (oxygen, nitrogen) inside a single-walled carbon nanotube [23]. The samples were irradiated to integral fluences 1.2×10^{17} and 1.6×10^{17} electron/cm^2. Thermal effects can be observed when nanotubes are irradiated with high energy electrons to high doses. However in order to eliminate the thermal effects in samples, they were irradiated at small current and frequent stoppages. Then some relative changes were checked whether they are present or absent. Samples were inspected 1 hour after irradiation, 1 day after, 1 month and 5 months after and no change was observed [14].

The SWCNTs were characterized by Raman spectroscopy (Renishaw in Via Raman microscope) using a 532 nm laser excitation source operated at 10 mW over a range 100–3200 cm^{-1} and using a 1800 I/mm(vis) grating. The XRD technique (Panalytical Empyrean 3) was used to characterize structure of SWCNT following modes: X-ray voltage 40.0 kV, current 45.0 mA, scanning range $2\theta_B$ = 20°–120°, scanning speed 2 deg/min and step size 2θ= 0.013°.

III. Experimental results and discussion

III.1. X-ray diffraction

The diffraction patterns were obtained from the raw XRD spectra by treatment with the Ritveld method using the Fullprof program (Fig. 1.).

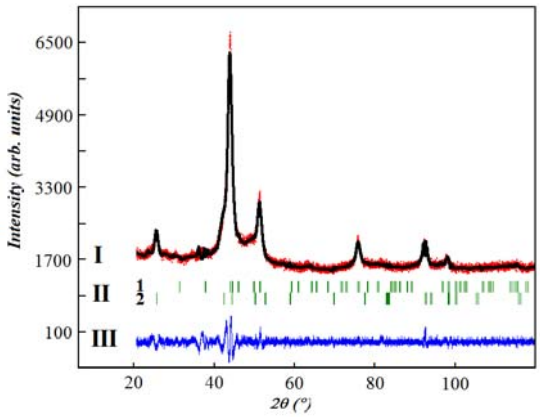

Figure 1. X-ray diffraction pattern of initial SWCNT structure. I – the difference between experimental and fitted data, II – the peaks was found calculation, III – comparison of the experimental data with the fitted data using the resolution function of the diffractometer.

Many space groups (Fd $\bar{3}$m, P6$_3$/mmc, P6$_3$/mc, P6/mmm, R $\bar{3}$m) were studied and it was found space group of SWCNT sample. SWCNT space group consist of two phases: P6/mmm and P6$_3$/mc (χ^2=2.09). When the sample was analyzed as single-phase the χ^2 (Bragg contrib.) was 10.7, the Bragg *R*-factor was 82.3, R_F-factor was 92.2.

The samples were irradiated with 1.18×10^{17} and 1.54×10^{17} electron/cm^2 fluency and the structure parameters were calculated (Tabl. 1).

Table 1. Initial and irradiated cell parameters of SWCNT. Phase 1 is SWCNT and Phase 2 is graphite.

Fluence, electron/cm^2	*a, b* (Å)		*c* (Å)	
	Phase1	Phase2	Phase1	Phase2
0	4.7623	2.4630	3.9491	6.9538
1.18×10^{17}	4.8286	2.4647	3.9394	6.8383
1.54×10^{17}	4.9378	2.5022	3.9469	6.9878

At $2\theta_B$=44° 2 phases correspondent, (200) and (111) Bragg peaks from the first phase, (101) peak from the second phase (Fig. 2, top). The (111) and (101) peak intensity share are equal 0.

After different by high e-beam irradiation all the experimental XRD patterns were compared and only (200) diffraction peaks was clearly decreased and shifted to higher angles with increasing the irradiation fluence, which can be summarized as the nanoparticle size growth (Fig. 2, bottom).

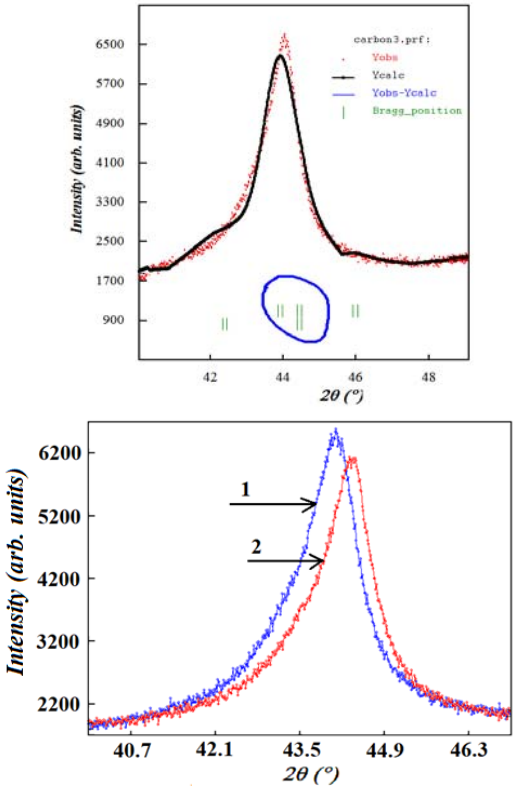

Figure 2. The XRD patterns of the initial (1) and irradiated (2) samples at the reflection (002).

© Academy of Sciences of Republic of Uzbekistan, 2021

C-C bond lengths of SWCNT was calculated (Tabl. 2) using the Fullprof program.

Table 2. C-C bond lengths of SWCNT for pristine and post irradiation sample.

Fluence, electron/cm^2	$a_{C1\text{-}C2}$, Å	$a_{C1\text{-}C3}$, Å	$a_{C1\text{-}C4}$, Å
0	1.453	2.749	3.109
1.54×10^{17}	1.452	2.851	3.199

III.2. Raman scattering

The radial breathing mode(RBM) bands are a useful diagnostic tool for confirming the presence of SWCNTs as well as depend on chirality and diameter of SWCNTs. The RBM frequency is inversely proportional to the diameter of the tube, making it an important feature for determining the diameter distribution in a sample and calculated using the expression $\omega_{RBM}=A/d_t+B$, where A and Bare determined experimentally [6], in [24] authors choice has a very good quantitative agreement with other calculations

$$\omega_{RBM} = \frac{227}{d_t}\sqrt{1 + C_{env} d_t^2 (1)}\ , \qquad (1)$$

where C_{env} quantifies the effect of the environment on the RBM frequency and for most samples in the literature present 0.056 nm^{-2} [24]. The RBM bands of SWCNT were observed at 169 cm^{-1} and 168 cm^{-1} for pristine and post irradiation accordingly. From the (1) equation was calculated the value of d_t: 1.42 nm for pristine sample (Fig. 3a), 1.43 nm for irradiation sample at 1.54×10^{17} electron/cm^2 (Fig. 3b).

According to the nanotube diameters found through the RBM bands, the chiral indices of the nanotube were found to be for the pristine (18,0) and for the post-irradiated (15,5) [25]. Armchair type is always metallic (n=m) and the other two types, Zigzag (n=0 or m=0) and Chiral ($n\neq m$) can be either metallic or semiconductor depending on their chiral condition [26]. If ($n-m$) is divisible by 3 then the tube is metallic and if ($n-m$) is not divisible by 3 then the tube is a semiconductor. From this dependence it can be said that the pristine sample is a metal, the irradiated sample is a semiconductor.

As seen in RBM spectra distinct spectral intensity decrease was observed.

The G band is a tangential share mode of carbon atoms that corresponds to the stretching mode in the graphite plane [13] and depends on whether the nanotube is semiconducting or metallic [17]. Raman spectra showed the G band at 1582 cm^{-1} for pristine sample (Fig. 3a). After 1.6×10^{17} electron/cm^2 fluence G peak was shifted to 1591 cm^{-1} and intensity was decreased (Fig. 3b). The asymmetry of the G peak (before and after electron irradiation) indicates that the given spectrum consists of G^+ and G^- bonds, where G^+ (corresponds to transverse vibrations of carbon atoms) is associated with charge transfer, and G^- (corresponds to longitudinal vibrations of carbon atoms) is due to metallic or semiconducting conductivity of a single-walled carbon nanotube.

One of the important results of this work is the shift in the wave number of the G mode from 1582 cm^{-1} in the initial state to 1591 cm^{-1} after irradiation with electrons. It is known that the value of 1582 cm^{-1} of the G mode corresponds to metallic conductivity [19], and its change to 1591 cm^{-1} may indicate the semiconducting nature of the conductivity [19].

The D band is a longitudinal optical phonon and is known as a disordered or defect (such as heteroatoms, vacancies, heptagon-pentagon pairs, kinks or even the presence of impurities, etc.) mode because a defect is required to elastically scatter in order for the process to conserve momentum [12]. The D band peaks were observed at the position 1331 cm^{-1} (Fig. 3a) and 1337 cm^{-1} (Fig. 3b) for pristine and post-irradiation accordingly. The D band intensity after electron irradiation clearly increased is shown was appeared radiation damages (Fig. 3a, 3b).

The G′ band frequency is close to twice that of the D band and is found from 2500 to 2900 cm^{-1}. This is a second-order process from two zone boundary LO phonons. The G′ band is an intrinsic property of the nanotube and graphite, and present even in defect-free nanotubes for which the D band is completely absent [14]. G′ band peaks to appear at 2653 cm^{-1} and 2665 cm^{-1} for pristine and post irradiation accordingly.

The electron irradiation increased intensity ratio of I_D/I_G from 0.04 to 0.26. The intensity ratio can directly serve as a measure of CNT structural quality, that is, the quality of the single-walled nanotube has deteriorated.

The nanocrystallite size of the SWCNT has enlarged [15] with the 1.54×10^{17}electron/cm^2 fluence, respectively and can see that by using Scherrer equation (2).

© Academy of Sciences of Republic of Uzbekistan, 2021

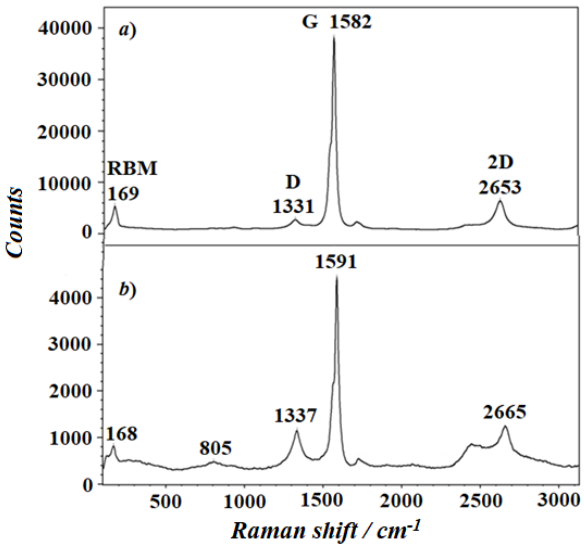

Figure 3. Raman spectra of SWCNT: *a*) pristine, *b*) at 1.6×10^{17} electron/cm^2 fluence.

$$D = \frac{k\lambda}{\beta_S \cos\theta}. \qquad (2)$$

Here, D is nanocrystallite size, which may be smaller or equal to the grain size; k is a dimensionless shape factor, has a typical value ~0.9; λ is the X-ray wavelength; β_S is the band width broadening at half the maximum intensity associated with microstress, in radians, θ is the Bragg angle.

The formula (2) does not take into account the presence of microstrain in the samples; therefore, the dimensions of the coherent scattering regions in highly deformable samples are not suitable for calculations.

For this, there is the Stokes formula:

$$\beta_D = 4\varepsilon \mathrm{tg}\theta, \qquad (3)$$

here ε is the value of the relative strains of the crystal lattice.

Taking into account that irradiation with high energy electrons can lead to the appearance of microstrain in the sample, full width at half maximum (β) of the experimental peaks can be represented as the sum of the peak width due to microstrain (β_s) and the peak width associated with grain size (β_D), i.e.

$$\beta = \beta_S + \beta_D. \qquad (4)$$

For this, we used the full width of the peaks at half maximum and the integral intensities of the reflections from 1 phase (200), (102), (103) and (222), from 2 phase (002) and (200).

D_{in}= 4.06 nm ($\varepsilon=8.42\times10^{-3}$)

$D_{1.18}$= 4.09 nm ($\varepsilon=8.11\times10^{-3}$)

$D_{1.54}$= 5.03 nm ($\varepsilon=7.62\times10^{-3}$)

Structure analysis of SWCNT showed the lattice parameters were enlarged, the reason for these changes were vacancies created by energetic electrons. This mechanism was invoked by [21, 22] and explain follow: the vacancies of SWCNT gave rise to surface reconstructions and diameter got larger because of appeared double vacancy (DV) transforms to an aggloration of five- and eight-membered rings (Fig. 4).

Therefore carbon nanotubes can be called self-healing materials.

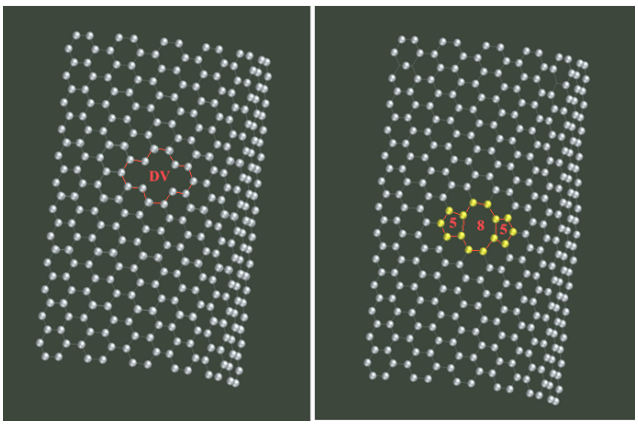

Figure 4. SWCNT defects reconstructions. Double vacancy (DV) transforms to an agglomeration of five- and eight-membered rings in C-C bonds.

Thus, irradiation of a single-walled carbon nanotube with electrons up to fluence of 1.54×10^{17} electron/cm^2 can be and stimulates the transition from metallic to semiconducting conductivity. It could be assumed that the increase in the intensity of the D-mode after electron irradiation is associated with an increase in the content of amorphous carbon. However, the width of the peak in Raman spectroscopy is less than ≈100 cm^{-1}, and also in the X-ray diffraction pattern at small scattering angles, there is no broad diffuse peak (halo) characteristic of amorphous carbon.

All this indicates that irradiation does not promote the formation of amorphous carbon in a SWCNT, but indicates the formation of other types of defects (breaking of the C-C bond).

© Academy of Sciences of Republic of Uzbekistan, 2021

IV. Conclusion

It was found that the initial sample of a single-walled carbon nanotube is two-phase with hexagonal phases with the space group P6/mmm and $P6_3/mc$.

Irradiation with electrons up to a fluency of 1.54×10^{17} electron/cm^2 leads to an increase in the lattice parameter a and b from 4.7623 Å to 4.9378 Å and a decrease in the parameter c from 3.9491 Å to 3.9469 Å.

Radiation treatment with electrons fluency of 1.54×10^{17} electron/cm^2 leads to an increase in the size of nanocrystallites from 4.06 nm to 5.03 nm, as well as a decrease in microstrain with an increase in the electron fluence.

Irradiation of a SWCNT with electrons energy of 2 MeV to the fluence of 1.54×10^{17} electron/cm^2 does not contribute to an increase in the graphite content in the SWCNT.

The value of the diameter of the SWCNT d = 1.42 nm after electron irradiation with a fluence of 1.54×10^{17} electron/cm^2 indicates a weak effect of radiation on the initial nanotube diameter d = 1.43 nm. The (n, m) integers of nanotube was determined to be (18, 0) and (15, 5), pristine and post irradiation, respectively, and after irradiation the nanotube was transferred from the metal to the semiconductor state. This is also proved by the fact that the G mode frequency is shifted to the right.

A Raman spectrum was found at 805 cm^{-1}, which is due to the formation of defects induced by electron irradiation with a fluence of 1.54×10^{17} electron/cm^2.

It was found that electron irradiation leads to deterioration of the I_D/I_G quality of a single-walled carbon nanotube from 0.04 to 0.26. The C-C bonds after irradiation were decreased.

Acknowledgment. We would like to thank colleagues “Electronica U003” accelerator for help irradiating progress. Also we thank V.M. Rotshteyn to measure Raman spectroscopy.

This research was carried out under themes of Institute of Nuclear Physics of Academy of Sciences of the Republic of Uzbekistan "Radiation-stimulated processes in nuclear transmutation in alloyed silicon single crystals".

References

[1] A. Aqel, Kh.M.M. Abou El-Nour, R.A.A. Ammar, A. Al-Warthan. Arabian Journal of Chemistry **5**, 1-23 (2012).

[2] A. Eatemadi, H. Daraee, H. Karimkhanloo, M. Kouhi et al. Nanoscale Research Letters **9**, 393 (2014).

[3] J. Maultzsch, H. Telg, S. Reich, and C. Thomsen, Phys. Rev. B 72, 205438 (2005). A. Firstauthorname, B. Secondauthorname, and C. Thirdauthorname, Here Goes the Title of the Book (Publisher, City, year), p. 111.

[4] A. Jorio, R. Saito, J.H. Hafner, C.M. Lieber, M. Hunter, T. McClure, G. Dresselhaus, and M.S. Dresselhaus. Phys. Rev. Lett. **86**, 1118 (2001).

[5] J.H. Choi, J. Lee, S.M. Moon, Y.T. Kim, H. Park, Ch.Y. Lee. J. Phys. Chem. Lett. **7**, 4739-4743 (2016).

[6] C. Kramberger, R. Pfeiffer, H. Kuzmany, V. Zólyomi, and J. Kürti. Phys. Rev. B **68**, 235404 (2003).

[7] A.M. Rao, E. Richter, S. Bandow, B. Chase, P.C. Eklund, K.A. Williams, S. Fang, K.R. Subbaswamy, M. Menon, A. Thess, R.E. Smalley, G. Dresselhaus, and M. S. Dresselhaus. Science **275**, 187 (1997).

[8] J. Kürti, G. Kresse, and H. Kuzmany, Phys. Rev. B **58**, R8869 (1998).

[9] L. Henrard, E. Hernandez, P. Bernier, and A. Rubio, Phys. Rev. B **60**, R8521 (1999).

[10] E.M. Dahl. Thesis submitted to the faculty of the Virginia Polytechnic Institute and State University in partial fulfillment of the requirements for the degree of Master of Science, Blacksburg, VA (2013).

[11] Y. Miyata, K. Mizuno, and H. Kataura. Journal of Nanomaterials **2011**, Article ID 786763, 7p. (2010).

[12] A. Jorio, A.G. Souza Filho, G. Dresselhaus, M.S. Dresselhaus, et al. Materials Research Society **706**, (2002).

[13] R. Saito, A. Gruneis, Ge.G. Samsonidze, V.W. Brar, et al, New Journal of Physics **5**, 157.1–157.15 (2003).

[14] I.I. Yuldashova, M.Y. Tashmetov. Physica B: Condensed Matter **571**, 280-284 (2019).

[15] M.A. Dresselhaus, G. Dresselhaus, R. Satio, and A. Jorio. Phys. Rep. **409**, 47-99 (2004).

[16] R.R. Bacsa, A. Peigney, C. Laurent, P. Puech, and W.S. Bacsa. Phys. Rev. B **65**, 161404R (2002).

[17] S. Costa, E. Borowiak-Palen, M. Kruszynska, A. Bachmatiuk, R.J. Kalenczuk, Material Science-Poland **26**, No.2 (2008).

[18] J. Park, S.J. Shin and M.J. Seong, Journal of the Korean Physical Society **53**, No.4, 2312-2315 (2008).

[19] A. Jorio et al, New Journal of Physics **5**. No.1, 139 (2003).

[20] Ch.H. Kiang, W.A. Goddard, R. Beyers, and D.S. Bethune, J. Phys. Chem. **100**, 3749-3752 (1996).

[21] A.V. Krasheninnikov, K. Nordlund. Nuclear Instruments and Methods in Physics Research B **216**, 355-366 (2004).

[22] A.V. Krasheninnikov and F. Banhart. Nature Materials **6**, No.10, 723-733 (2007).

[23] Y. Maniwa et al. Jpn. J. Appl. Phys. **38**, L668 (1999).

[24] A. Jorio and R. Saito. Raman spectroscopy for carbon nanotube applications. Journal of Applied Physics **129**, 021102 (2021).

[25] [http://www.photon.t.u-tokyo.ac.jp/~maruyama/kataura/chiraldata.html]

[26] C. Thomsen and S. Reich. Raman scattering in carbon nanotubes. Top. Appl. Phys. **108**, 115-232 (2007).

© Academy of Sciences of Republic of Uzbekistan, 2021

Юқори энергияли электронлар дастаси таъсири остидаги бир деворли углерод нанонайчалар структураси ва радиациявий нуқсонлар

М.Ю. Ташметов, И.И. Юлдашева

Ўзбекистон республикаси Фанлар академияси Ядро физикаси институти, Мирзо-Улуғбек тумани, Улуғбек қўрғони, Хуросон кўчаси 1-уй, 100214,Тошкент, Ўзбекистон

Бир деворли углерод нанонайчалар (БДУНН) структура параметрларига, нанокристаллитлар ўлчамига, микрокучланишига ва комбинацион сочилиш спектрларига 1.54×10^{17} электрон/см^2 флюенсгача электронлар билан нурлантиришнинг таъсири тадқиқ қилинди. Электронлар билан нурлантириш панжара параметрларининг *a* ва *b* йўналишларда 4.7623 дан 4.9378 Å гача ортишига ва *c* ўқ бўйича 3.9491 дан 3.9469 Å гача олиб келди. Электрон билан нурлантириш бир деворли углерод нанонайчаларда нуқсонлар ҳосил бўлиши туфайли нанокристаллитлар ўлчамини 4.06 нм дан 5.03 нм гача ўсишига ва комбинацион сочилиш спектрларини юқори частота томонга силжишига олиб келди ҳамда 805 см$^{-1}$ спектри ҳосил бўлишини кўрсатди.

Калит сўзлар: бир деворли углерод нанонайчалар, электронлар дастаси, Раман спектроскопияси, рентген структуравий таҳлил, катак параметрлари.

© Academy of Sciences of Republic of Uzbekistan, 2021